4. CONCLUSIONS

In summary, CMOS compatible ICP deep trench technology is used to remove the silicon underneath a monopole antenna implemented in 0.18-μm CMOS process. The experimental results show that the input return losses can be improved by as large as 5 dB and power transfer ratio can be increased from 0.87 to 0.96 because of the reduction of dielectric losses by ICP etching. Therefore, high-performance fully integrated silicon MMICs including antennas can be expected with the help of this ICP technology.

ACKNOWLEDGMENTS

The authors thank the National Chip Implementation Center and UMC for IC implementation and the National Nano-Device Laboratory for measurement supports. Financial supports from national science council under contract no. NSC 97-2221-E-002 -153 -MY3 and no. NSC 99-2218-E-182-010 are also appreciated.

REFERENCES

1. C.H. Doan, S. Emami, A.M. Nikenejad, and R.W. Broadersoen, Millimeter-wave CMOS Design, IEEE J Solid-State Circuits 40 (2005), 144–155.
2. K.K.O, K. Kim, B.A. Floyd, J.L. Mehta, H. Yoon, C.-M. Hung, D. Bravo, T.O. Dickson, X. Guo, R. Li, N. Trichy, J. Caserta, W.R. Bomstad, II, J. Branch, D.-J. Yang, J. Bohorques, E. Seok, L. Gao, A. Sugavanam, J.-J. Lin, and J. E. Brewer, On-chip antenna in silicon ICs and their application, IEEE T Electron Devices 52 (2005), 1312–1323.
3. B. Rong, J.N. Burghartz, L.K. Nanver, B. Rejaei, and M. van der Zwan, Surface-passivated high-resistivity silicon substrates for RFICs, IEEE Electron Device Lett 25 (2004), 176–178.
4. I.-Y Chen, C.-U. Huang, H.J.H. Chen, C.F. Jou, and R.-S. Huang, A 2.4 GHz and 5.2 GHz dual-band antenna fabricated on flexible parylene membrane, Jpn J Appl Phys 44 (1997), 8356–8361.
5. I.K. Itotia and R.F. Drayton, Porosity effects on coplanar waveguide porous silicon interconnects, IEEE MTT-S Digest 2002, pp. 681–684.
6. M.T. Yang, T.J. Yeh, H.M. Hsu, P.C. Ho, Y.J. Wang, Y.T. Chia, and D.D.L. Tang, Characterization and model of high quality factor and broadband integrated inductor on Si-substrate, IEEE MTT-S Digest 2003, 1283–1286.
7. T. Wang, Y.-S. Lin, and S.-S. Lu, An ultralow-loss and broadband micromachined RF inductor for RFIC input-matching applications, IEEE T Electron Devices 53 (2006), 568–570.
8. T. Wang, C.-H. Chen, Y.-S. Lin, and S.-S. Lu, A micromachined CMOS distributed amplifier by CMOS compatible ICP deep-trench technology, IEEE Electron Device Lett 27 (2006), 291–293.
9. T. Wang, H.-C. Chen, H.-W. Chiu, Y.-S. Lin, G. W. Huang, and S.-S. Lu, Micromachined CMOS LNA and VCO by CMOS-compatible ICP deep trench technology, IEEE T Microwave Theory Tech 54 (2006), 580–588.
10. W.L. Stutzman and G.A. Thiele, Antenna theory and design, 2nd ed., Wiley, New York, NY, 1998, p. 220.

A 3.4/5.5 GHZ DUAL-BAND NOTCHED UWB PRINTED MONOPOLE ANTENNA WITH TWO OPEN-CIRCUITED STUBS IN THE MICROSTRIP FEEDLINE

Jyoti Ranjan Panda and Rakhesh Singh Kshetrimayum
Department of Electronics and Electrical Engineering, Indian Institute of Technology Guwahati, 781039, India; Corresponding author: krs@iitg.ernet.in

Received 8 March 2011

ABSTRACT: *An ultrawideband (UWB) printed monopole antenna (PMA) for the 3.4/5.5 GHz dual-band notched operation is presented. The antenna has a rectangular radiating element with a symmetrical staircase structure in the bottom or feed region and fed by a 50-Ω microstrip line. By introducing two open-circuited stubs from the two sides of the microstrip feedline, dual band-notched characteristics in the WiMAX/WLAN bands are achieved. The proposed antenna is effectively designed, simulated, fabricated, and measured providing broadband impedance matching, appropriate gain, and stable radiation pattern characteristics. An UWB and single band-notched UWB antenna are also fabricated for comparison. The proposed UWB antenna is investigated in time domain, and it has been observed experimentally that the received fifth derivative of Gaussian pulse is not distorted in the main waveform but some amount of ringing is observed.* © 2011 Wiley Periodicals, Inc. Microwave Opt Technol Lett 53:2973–2978, 2011; View this article online at wileyonlinelibrary.com.
DOI 10.1002/mop.26380

Key words: *band-notched characteristics; microstrip line; open-circuited stubs; UWB antenna*

1. INTRODUCTION

Federal Communication Commission's (FCC)'s ruling in February 2002 [1] for the commercial use of huge band from 3.1 to 10.6 GHz has completely revolutionized the wireless and high speed data communication world. This huge bandwidth from 3.1 to 10.6 GHz is assigned as the ultrawideband (UWB) spectrum by FCC. But along with the vast operating bandwidth of the UWB antenna (3.1–10.6 GHz), there exist some narrowband (NB) wireless services, which occupy some of the frequency bands in the UWB bands. The most well known among them is wireless local area network (WLAN) IEEE802.11a and HIPERLAN/2 WLAN operating in 5–6 GHz band. Apart from WLAN, in some European and Asian countries, world interoperability for microwave access (WiMAX) service from 3.3 to 3.6 GHz also shares spectrum with the UWB. In some antenna designs, the UWB antenna uses filters to notch out the interfering bands. However, the use of filters increases the complexity of the UWB system and also increases the weight and size of the UWB transreceivers. Hence, it has been necessitated to design UWB antenna with dual band-notched characteristics both in 3.3–3.6 GHz and 5–6 GHz to mitigate the interference between the narrowband wireless systems and UWB systems. Till now, many designs of the UWB band-notched antennas are proposed to alleviate the disturbance caused by the WLAN with the UWB system.

Based on the background of the structures of various UWB notch-antennas [2–7], this letter proposes a simple and compact microstrip line fed UWB PMA (2.63–13.1 GHz) with dual band-notched characteristics in 3.48 GHz (3.03–4.04 GHz) and 5.59 GHz (4.76–6.29 GHz). The dual band-notched characteristic in the proposed antenna has been achieved by introducing two open-circuited stubs from the two sides of the microstrip feedline. By adjusting the length of the two open circuited stubs approximately to one quarter of the guided wavelength (λ_g) of the required notch frequency, a destructive interference of the current distribution takes place causing the antenna nonradiating at that notch frequency. The tuning of the central notch frequency can be done suitably by adjusting the total length of the two open-circuited stubs. The optimization of the design and the subsequent simulation is done using IE3D software [8]. The proposed antenna provides measured impedance bandwidth of 3.1–10.6 GHz with VSWR $\leq$ 2, except the bandwidths of 3.03–4.04 GHz for WiMAX systems and 4.76–6.29 GHz for IEEE802.11a and HIPERLAN/2 WLAN systems. The appropriate gain and stable radiation patterns are also observed experimentally.

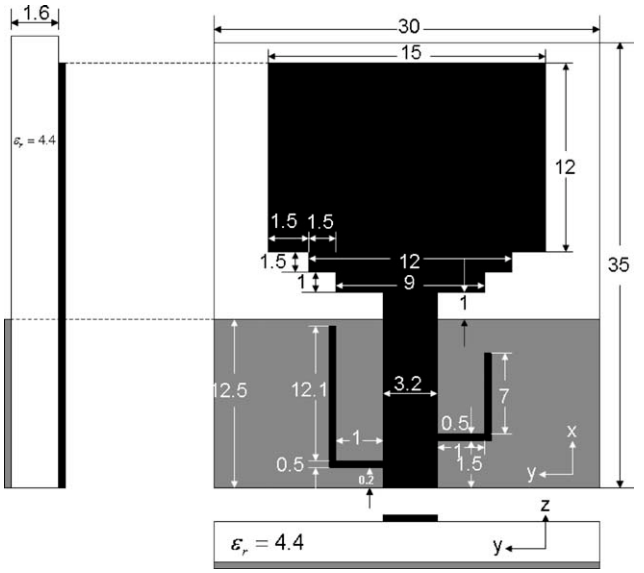

Figure 1 Geometry of antenna 3

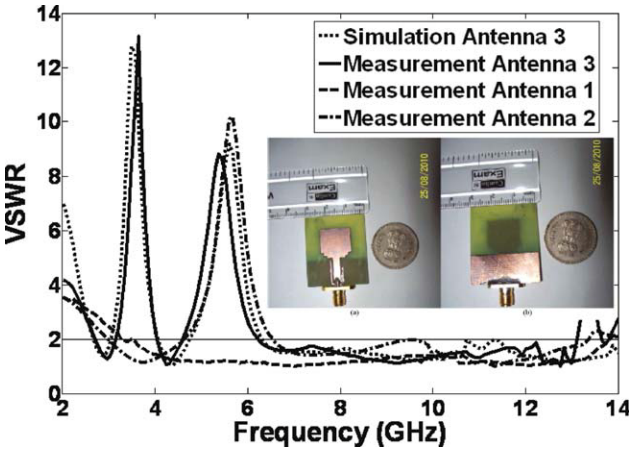

Figure 2 Measured and simulated VSWR of antenna 3, compared to measured VSWR of antenna 1 (UWB antenna) and antenna 2 (Single band-notched antenna). [Color figure can be viewed in the online issue, which is available at wileyonlinelibrary.com]

In this letter, a compact UWB PMA of area 30 × 35 mm^2 is proposed. Open-circuited stubs on two sides of the microstrip feedline create dual band-notched characteristics for coexistence without interference between the NB and the UWB wireless systems. Detailed time and frequency domain simulation as well as experimental results along with a brief discussion on the antenna designs are presented to demonstrate the performance of the proposed antenna.

2. UWB DUAL BAND-NOTCHED ANTENNA DESIGN AND RESULTS

Figure 1 shows the geometry and configuration of a UWB dual-band notched antenna. The antenna (referred to as antenna 3 in this letter) was fabricated on an $h = 1.6$ mm FR4 epoxy substrate with the dielectric constant $\varepsilon_r = 4.4$ and loss tangent tan $\delta = 0.002$. As shown in the figure, the shape of the radiating element is rectangular, and there is a stair case structure symmetrically the two bottom corners of the radiating element. The design parameters are given in the Figure 1. The staircase structure improves the impedance matching and the bandwidth of the antenna 3. The fabricated prototype of antenna 3 is shown inside the Figure 2. By introducing two open-circuited stubs on the both side of the microstrip feedline, the appropriate dual band-notched function both in 3.3–3.6 GHz and 5–6 GHz are achieved. The open circuited stub on the left side of the microstrip feedline provides the notch band at 3.4 GHz and the open circuited stub on the right side of the microstrip feedline provides another one at 5.5 GHz, each of the total length of the open-circuited stubs are approximately one quarter the guided wavelength (λ_g) of the required notch frequency.

The guided wavelength (λ_g) at 5.5 GHz was found to be 33.95 mm. By simulation the total length of the right side open circuited stub (L) was found to be $L = (1 + 0.25 + 0.25 + 7) = 8.5$ mm. Hence, the total length of the right-side open-circuited stub (L) is (8.5/33.95) = 0.25 times the guided wavelength (λ_g) of the desired notch frequency ($f_n = 5.5$ GHz). Similarly, λ_g at 3.48 GHz was found to be 67.25 mm. By simulation, the total length of the left-side open-circuited stub (L_1) was found to be $L_1 = (1 + 0.25 + 0.25 + 12.1) = 13.6$ mm. Hence, the total length of the left-side open-circuited stub (L_1) is (13.6/67.25) = 0.20 times the guided wavelength (λ_g) of the desired notch frequency ($f_n = 3.48$ GHz).

Figure 2 shows the measured and simulated VSWR of the antenna 3 compared to the measured VSWR of antenna 1 and antenna 2. The simulated VSWR graph of the antenna 3 provides two notches centered at 3.48 and 5.59 GHz, respectively. The frequency band at center notch frequency at 3.48 GHz (VSWR = 12.78) extends from 3.03 to 4.04 GHz and the frequency band at center notch frequency at 5.59 GHz (VSWR = 9.19) extends from 4.76 to 6.29 GHz. Similarly, the measured VSWR graph of the antenna 3 provides two notches centered at 3.63 and 5.37 GHz. The frequency band at center notch frequency at 3.63 GHz (VSWR = 13.15) extends from 3.15 to 4.02 GHz and the frequency band at center notch frequency at 5.37 GHz (VSWR = 8.81) extends from 4.58 to 6.20 GHz. The measured UWB extends from 2.63 to 13.1 GHz.

Figure 3 shows the variation of simulated and measured peak gain in dBi with the frequency for the UWB dual band-notched antenna 3 compared with the measured peak gain values for UWB antenna 1 and antenna 2. From the Figure, it is clear that there is sharp dip in the gain at around 3.30 and 5.5 GHz, which confirms that UWB dual band-notch antenna, becomes nonresponsive in the two-narrowband systems (WiMAX and WLAN).

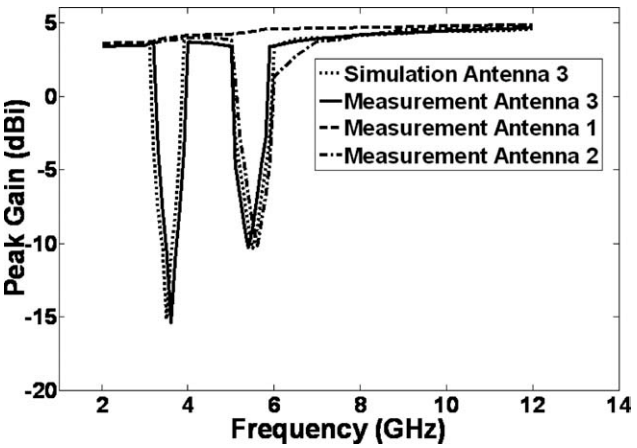

Figure 3 Measured and simulated peak gain (dBi) of antenna 3, compared with the measured peak gain of antennas 1 and 2

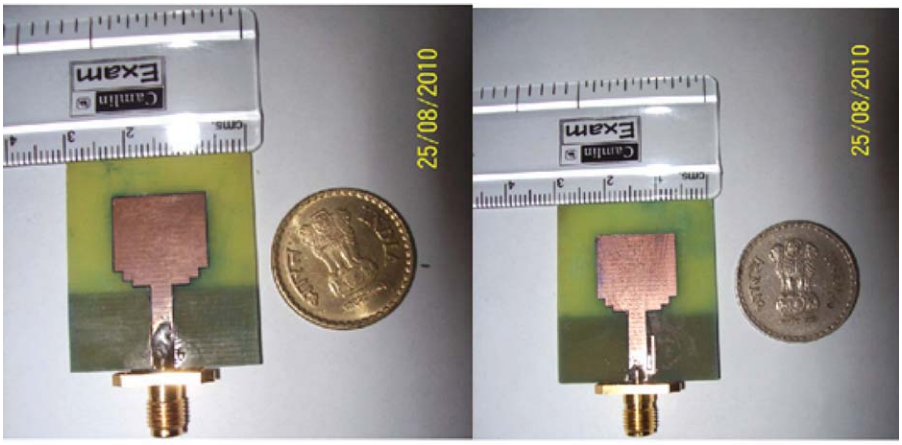

Figure 4 Fabricated prototype of the (a) UWB antenna (antenna 1) and (b) UWB single notch antenna (antenna 2). [Color figure can be viewed in the online issue, which is available at wileyonlinelibrary.com]

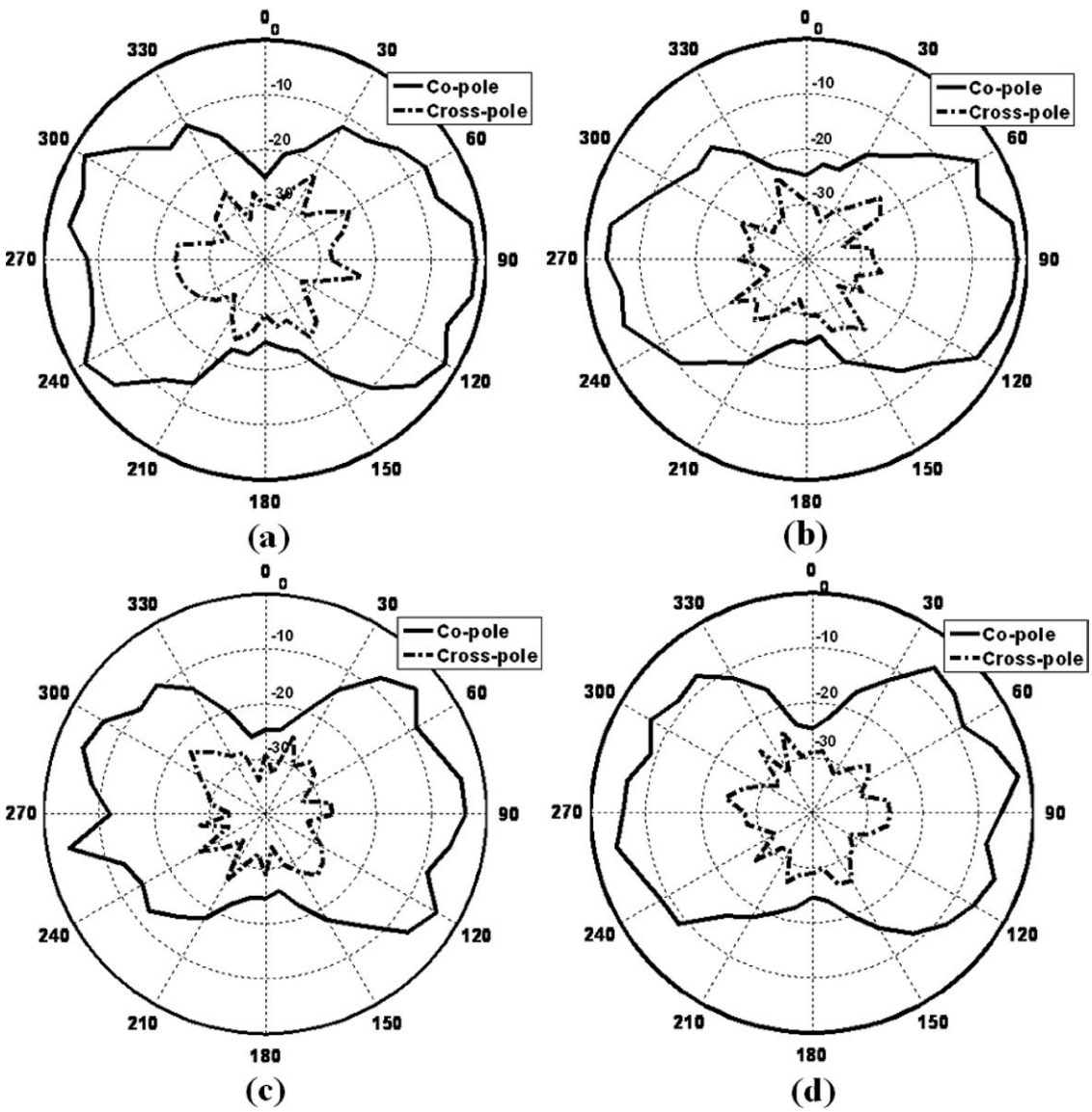

Figure 5 Measured *E*-plane (*xz*-plane) radiation patterns of UWB dual band-notch antenna (antenna 3) at (a) 4.5 GHz, (b) 7.5 GHz, (c) 9.5 GHz, and (d) 12 GHz

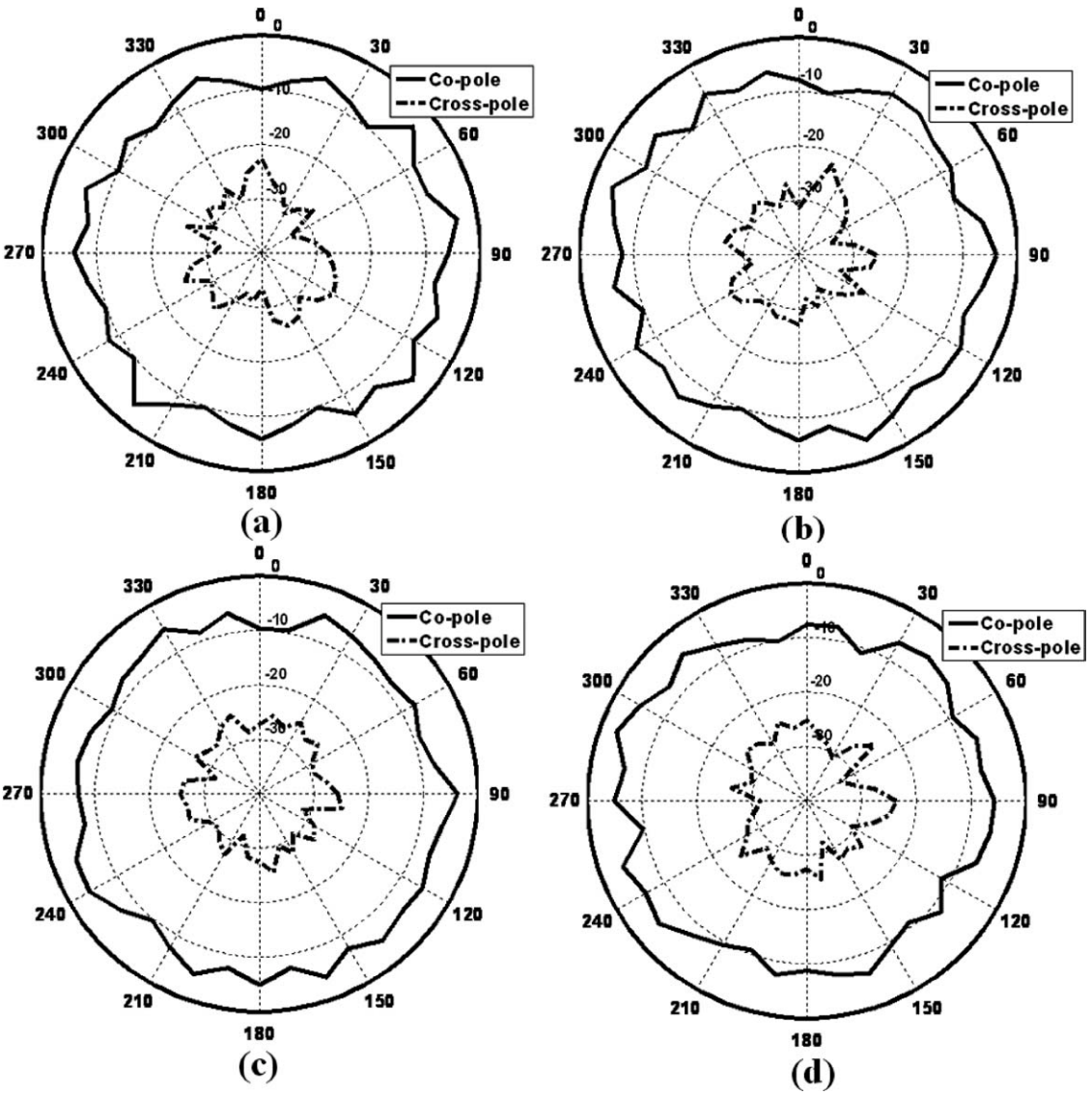

Figure 6 Measured *H*-plane (*yz*-plane) radiation patterns of UWB dual band-notch antenna (antenna 3) at (a) 4.5 GHz, (b) 7.5 GHz, (c) 9.5 GHz, and (d) 12 GHz

However, for the other frequencies outside the notched band, the antenna gain is appropriately consistent and almost stable in the whole of the UWB band. The measured peak gain of UWB dual band-notch antenna at 3.6 GHz is −15.35 dBi and at 5.4 GHz is −10.25 dBi, respectively. The top view of the fabricated prototype of the UWB antenna (antenna 1) and single band-notch UWB antenna (antenna 2) are shown in the Figures 4(a) and 4(b) respectively (the bottom view of these antennas are identical to that of antenna 3).

Figure 5 shows the measured normalized copolar and cross-polar *E*-plane (*xz*-plane) radiation pattern of the antenna 3 at 4.5, 7.5, 9.5, and 12 GHz, respectively, and Figure 6 shows measured normalized copolar and cross-polar *H*-plane (*yz*-plane) radiation pattern of the antenna 3 at 4.5, 7.5, 9.5, and 12 GHz, respectively. The copolar *H*-plane radiation pattern is purely omnidirectional at all the measured frequencies. The copolar *E*-plane radiation pattern is directional along 90° and 270°, respectively. In the copolar *E*-plane, the radiation patterns remain roughly a dumbbell-shape like a small dipole leading to bidirectional patterns. In case of both cross-polar *H*-plane and *E*-plane radiation patterns at 4.5, 7.5, 9.5, and 12 GHz, the radiation is in between −30 dB and −20 dB, showing not much energy radiation occurs in the cross-polar direction and more required radiation occurs in the copolar direction, making the proposed antenna an efficient radiator in the required direction.

3. TIME DOMAIN TRANSMISSION AND RECEPTION CHARACTERISTICS

In this letter, the UWB signal presented in [9] is used to excite the proposed antennas, which fulfills the FCC spectral mask and power spectral density (dBm/MHz) of antenna input signal (fif-the derivative of Gaussian pulse) combined for indoor systems shown inside Figure 7. The UWB pulse, which is used to excite the antennas is a fifth-order derivative of the Gaussian pulse and is given by

$$z_1(t) = \mathrm{GM}_5(t) = B\left(-\frac{t^5}{\sqrt{2\pi}\sigma^{11}} + \frac{10t^3}{\sqrt{2\pi}\sigma^{9}} - \frac{15t}{\sqrt{2\pi}\sigma^{7}}\right) \times \exp\left(-\frac{t^2}{2\sigma^2}\right) \quad (1)$$

where $B = 600$, is a constant which can be chosen to compatible with the peak power spectral density that the FCC permits

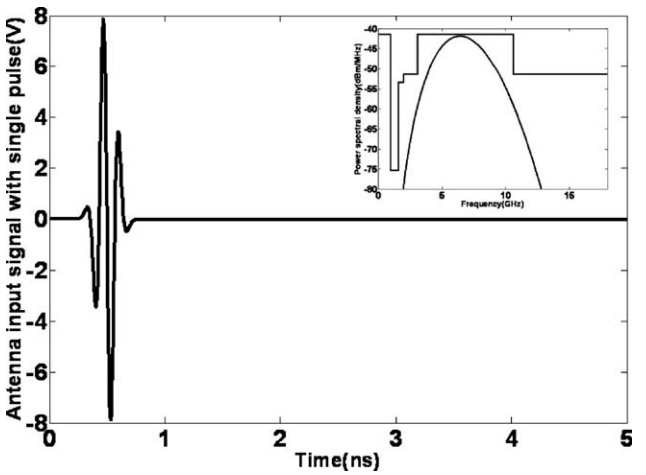

Figure 7 Antenna input signal (fifth derivative of Gaussian pulse) with single pulse

and σ is the spread of Gaussian pulse, whose value is 51 ns to ensure that the size and shape of the spectrum fit with the FCC mask. The signal with single pulse is shown in the Figure 8. The PSD of antenna input signal suitable fits the PSD of the FCC mask denoting the adequate compatibility of the fifth-order Gaussian pulse with the FCC indoor mask shown inside Figure 7.

Figure 8(b) shows the received pulse as the antenna 3 acts as a received antenna. The transmit antenna is also the replica of antenna 3. That means the fifth-order Gaussian pulse is transmitted from antenna 3 to antenna 3. The fifth-order Gaussian pulse is generated in Tektronix AWG 7122B arbitrary signal generator and it is fed to the transmit antenna 3. At 62 cm [10] away, the receiving antenna (antenna 3) stationed face-to-face. At the receiving side, the received signal is captured by Tektronix DPO 70804 digital phosphor oscilloscope. As from the Figure 8(b), there is ringing in the tail of the fifth-order Gaussian pulse, Apart from this, there is reduction in the amplitude of the received pulse. The reason for these two types of the disturbance in the received signal may be due to the noise and other disturbances present in the air channel in between the two antennas. Similarly, Figure 8(c) shows the above characteristics when the two antennas are place side-by-side. From Figures 8(b) and 8(c), one can see that the ringing in the tail of the received pulse is slightly more in case of side-by-side as compared to the ringing present in the received signal when the antenna placed face-to-face. This is because, when the antennas are stationed face-to-face, the whole of the radiating surface is exposed to receiving signal. This is the broadside direction of the radiation pattern. Hence the signal reception is smooth in this situation. But when the antennas are placed side-by-side, the radiation is in the end fire direction and no radiation pattern lobes are present to capture the receiving signal. So more ringing is present in the tail of the received signal.

4. CONCLUSIONS

To mitigate the potential interference between the UWB systems and NB systems such as WiMAX and WLAN, an UWB PMA with two open-circuited stubs in two sides of the microstrip feedline for the 3.4/5.5 GHz dual-band notched characteristics has been proposed. The relationship between the total dimension of the two open-circuited stubs and the notch band center frequency has been presented. Stable radiation pattern and constant gain in the UWB bands are obtained. The UWB PMA presented

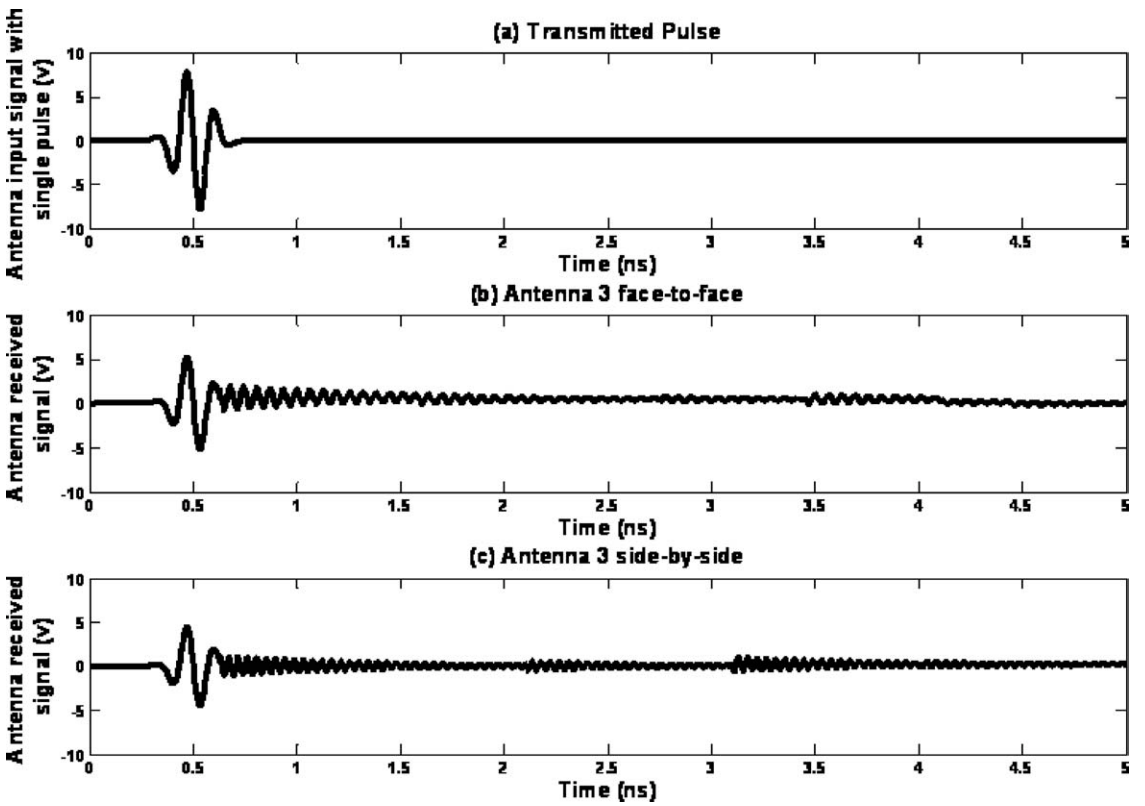

Figure 8 Measured received signals of antenna 3 as antenna 3 serve as the receiving antennas with single pulse input signal (a) transmitted Gaussian pulse, (b) antenna 3 face-to-face, and (c) antenna 3 side-by-side

in this letter is expected to find future applications in UWB systems for coexistence with the NB systems.

ACKNOWLEDGMENTS

The authors thank U. K. Sarma and D. Goswami of IIT Guwahati, G. Hemanth and Hemalatha of IISc Bangalore for their assistance in fabrication and measurements of the proposed antennas. Second author is grateful to Dr. K. J. Vinoy of IISc Bangalore and Prof. A. Mahanta of IIT Guwahati for allowing the first author to use their laboratories for various measurements of the proposed antennas.

REFERENCES

1. First Report and Order, Revision of Part 15 of the Commission's Rule Regarding Ultra-Wideband Transmission systems FCC 02–48, Federal Communication Commission, 2002.
2. R. Zaker, C. Ghobadi, and J. Nourinia, Novel modified UWB planar monopole antenna with variable frequency band-notch function, IEEE Antenna Wireless Propagat Lett 7 (2008), 112–114.
3. J. Liu, S. Gong, Y. Ku, X. Zhang, C. Feng, and N. Qi, Compact printed ultra-wideband monopole antenna with dual band-notched characteristics, Electron Lett 44 (2008), 710–711.
4. H. Lee, Y. Jang, J. Kim, and J. Choi, Wideband monopole antenna with WLAN (2.4 GHz/5 GHz) dual band-stop function, Microwave Opt Technol Lett 50 (2008), 1646–1649.
5. F.-J. Wang, X.-X. Yang, J.-S. Zhang, G.-P. Guo, and J.-X. Xiao, A band-notched ring monopole antenna, Microwave Opt Technol Lett 50 (2008), 1882–1884.
6. Z. Cui, Y.-C. Jiao, L. Zhang, and F.-S. Zhang, The band-notch function for a printed ultra-wideband monopole antenna with E-shaped slot, Microwave Opt Technol Lett 50 (2008), 2048–2052.
7. Y.-D. Dong, W. Hong, Z.-Q. Kuai, and J.-X. Chen, Analysis of planar ultrawideband antennas with on-ground slot band-notched structures, IEEE Trans Antennas Propagat 57 (2009), 1886–1892.
8. IE3D version 10.2, Zeland Corp., Freemont, CA, USA.
9. H. Kim, D. Park, and Y. Joo, All-digital low power CMOS pulse generator for UWB signals, Electron Lett 40 (2004), 1534–1535.
10. N. Telzhensky and Y. Leviatan, Novel method of UWB antenna optimization for specified input signal form by means of genetic algorithm, IEEE Trans Antennas Propagat 54 (2006), 2216–2225.

INVESTIGATION OF AN ULTRA-WIDEBAND MICROSTRIP ANTENNA USING FINITE ELEMENTARY LINES APPROACH

S. Senouci,[1] A. Zerguerras,[2] J. Tao,[2] and T. H. Vuong[2]
[1] Département d'Electronique, Ecole Nationale Polytechnique, Alger, Algérie
[2] Laboratoire LAPLACE, ENSEEIHT-INP, Toulouse, France; Corresponding author: senouci@laplace.univ-tlse.fr or sadsenou@yahoo.fr

Received 8 March 2011

ABSTRACT: *This work presents an investigation, using the approach of finite elementary lines (FEL), of an ultra-wideband antenna. Two ways for expanding frequency band were combined: the electromagnetic coupling and the insertion of an air layer. A prototype of this antenna has been realized. A comparison between the antenna performance predicted by our approach and those provided by the high-frequency simulation structure (HFSS) software and those measured is presented. An impedance bandwidth of about 50% and directivity at the first resonance of about 9 dB were achieved. A satisfactory concordance between results of our approach and measures is observed. The novelty of this work lies in the treatment by the FEL method, for the first time, of singularities induced by the gap of coupling and the jump of width. The computing time consumed by the FEL approach is about 10 times less than that consumed by the HFSS software to analyze the same structure on the same number of point's frequency domain, the latter being 68 min.* © 2011 Wiley Periodicals, Inc. Microwave Opt Technol Lett 53:2978–2985, 2011; View this article online at wileyonlinelibrary.com. DOI 10.1002/mop.26379

Key words: *microstrip antennas; band expanding techniques; coupling; electromagnetic; coupling gap; width jump*

1. INTRODUCTION

The ultra-wideband (UWB) systems are defined as systems that use signals with bandwidths exceeding 500 MHz or a bandwidth of 20% around its central frequency. UWB systems provide higher rates for wireless communications, radar systems, and precise geo-location. The mistress component of these systems is the UWB antenna.

The microstrip antennas are usually based driver patch printed on a microwave dielectric substrate having a face completely covered with conductive metal, called ground plane. These antennas have several advantages such as low profile, low cost, light weight, easy fabrication, and conformability on curved surfaces. However, their major drawbacks are the small gain and the close frequency bandwidth, because in practice applications-based microstrip antennas require high gain and wide frequency bands.

Indeed, miniaturization of microstrip antennas, extending their frequency bands and increase their gains are operations required for some practical applications such as mobile cell phone wireless, direct broadcast satellite, the wireless LAN, satellite global positioning, and other future generations of wireless terminals.

These three operations are changing in meaning contradictory, that is to say, the miniaturization leads to a drop in gain and increase the gain adversely affects the band width; this leads to seek a compromise between the parameters of the antenna to achieve the desired performance for a specific application.

Widening the frequency band of a microstrip plate antenna (MPA) calls the use of substrates with low dielectric constant and high thickness [1–6]. But the excessive increase in thickness to improve bandwidth causes unwanted radiation and increases the power of surface waves contributing to the decrease in antenna efficiency. Therefore, a compromise between the dielectric constant, the thickness of the substrate and the bandwidth is taken into account during the synthesis of MPA.

The physical dimensions of the antenna are an important factor in the design process [7] to which is due the miniaturization of modern mobile phones. Much attention has been given to a technique for miniaturizing the dimensions of the MPA [8–12]. The electrical requirements of these mobile antennas are sufficient bandwidth, high efficiency, impedance matching, omnidirectional radiation patterns, and minimal degradation by the presence of objects in the immediate vicinity, and so on.

The bandwidth enlargement technique used in this letter is one that combines both techniques simultaneously, namely: first, the electromagnetic coupling between a patch excited by coaxial probe called driven patch and a patch coplanar with the first known as parasitic patch or director patch. A first enlargement is obtained by the juxtaposition of the two resonances of the two patches. The second technique is the inclusion of a layer of air between the ground plane and the substrate. The air layer